JACS
JOURNAL OF THE AMERICAN CHEMICAL SOCIETY

Communication

pubs.acs.org/JACS

Spherical Nanoparticle Supported Lipid Bilayers for the Structural Study of Membrane Geometry-Sensitive Molecules

Riqiang Fu,[§,⊥] Richard L. Gill, Jr.,[†,⊥] Edward Y. Kim,[‡] Nicole E. Briley,[†] Erin R. Tyndall,[†] Jie Xu,[†] Conggang Li,[∥] Kumaran S. Ramamurthi,[‡] John M. Flanagan,[†] and Fang Tian*[,†]

[†]Department of Biochemistry and Molecular Biology, The Pennsylvania State University, Hershey, Pennsylvania 17033, United States

[‡]Laboratory of Molecular Biology, National Cancer Institute, National Institutes of Health, Bethesda, Maryland 20892, United States

[§]National High Magnetic Field Laboratory, Tallahassee, Florida 32310, United States

[∥]National Center for Magnetic Resonance in Wuhan, Wuhan Institute of Physics and Mathematics, Chinese Academy of Sciences, Wuhan 430071, P. R. China

Supporting Information

ABSTRACT: Many essential cellular processes including endocytosis and vesicle trafficking require alteration of membrane geometry. These changes are usually mediated by proteins that can sense and/or induce membrane curvature. Using spherical nanoparticle supported lipid bilayers (SSLBs), we characterize how SpoVM, a bacterial development factor, interacts with differently curved membranes by magic angle spinning solid-state NMR. Our results demonstrate that SSLBs are an effective system for structural and topological studies of membrane geometry-sensitive molecules.

Biological membranes exhibit diverse shapes, and there is a growing body of evidence that membrane topology plays key roles in many cellular processes.[1,2] For example, cellular processes such as endocytosis, vesiculation, organelle synthesis, and cell division require transient membrane remodeling with a high degree of spatial and temporal accuracy. Further, entry of some bacteria and viruses into human cells also involves alteration of membrane structure.[3] Recently, it was discovered that the curvature of the membrane bilayer can regulate the enzymatic activity (e.g., human ArfGAP1, tafazzin),[4,5] and define the subcellular localization, of some proteins (e.g., bacterial development factors SpoVM and DivIVA).[6−8] Increasingly, membrane geometry is viewed as an essential component of a microenvironment for membrane fusion and fission, protein localization, trafficking, and signaling.[9,10] Membrane rearrangement is often governed by proteins that can sense and/or induce membrane curvature (e.g., BAR domain-containing proteins, dynamin, and epsins),[11] but our understanding of the underlying molecular mechanisms of these processes remains rudimentary. Specifically, how do membrane geometry-sensitive molecules detect differences in curvature and how curvature affects their structures and membrane topology? In part, this gap in understanding is due to a lack of high resolution structural information in native-like membrane environments having a wide-range of stable and precisely controlled curvature.

To date, liposomes are the most common system for the structural analysis of membrane proteins. While relatively homogeneous small (∼50 nm) and large unilamellar vesicles (∼100 nm) can be prepared to mimic highly curved membranes, the preparation of giant unilamellar liposomes (GUVs) has been difficult. GUVs are not stable and are usually polydisperse in size and degree of curvature, limiting their use in structural studies.[12] By contrast, spherical nanoparticle supported lipid bilayers (SSLBs),[13] first introduced in 1990, preserve many characteristics of cell membranes such as lateral fluidity, impermeability to ionic species, and flexibility along the fatty acyl chain. The absorbed lipids form a single bilayer and are separated from the solid supports by a thin layer of water molecules (∼20 Å, Figure 1). SSLBs can be prepared with well-defined curvatures (defined by the size of solid supports) and surface stiffness[14,15] and have been used in biophysical studies of several bilayer-interacting peripheral membrane proteins.[16,17] Here, we demonstrate the utility of SSLBs coupled with high-resolution magic angle spinning (HRMAS) solid-state NMR (ssNMR) for structural studies of membrane curvature-sensitive molecules. This system proves to be ideal for defining the role of membrane curvature in modulating protein−lipid interactions.

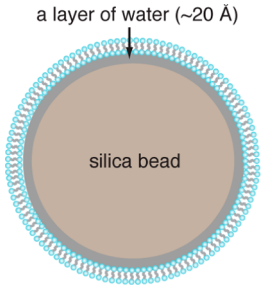

Figure 1. SSLB representation.

As an initial test system, we have examined the protein−lipid interaction of SpoVM. SpoVM is a small (26 residue) peripheral membrane protein from *Bacillus subtilis*.[18] Under nutrient-limiting conditions, *B. subtilis* initiates a developmental

Received: August 6, 2015
Published: October 21, 2015

DOI: 10.1021/jacs.5b08303
J. Am. Chem. Soc. 2015, 137, 14031−14034

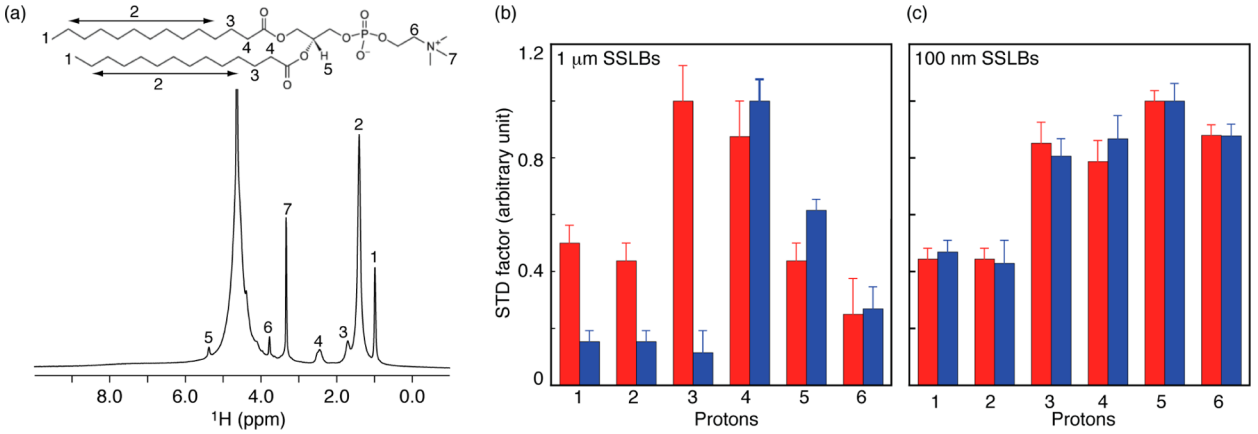

Figure 2. Curvature-dependent membrane insertion depth. (a) 1D 500 MHz ^{1}H HRMAS spectrum of DMPC-coated 1 μm SSLBs recorded at 30 °C, 10 kHz spinning speed. STD factors of SpoVM (red) and SpoVM^{R17D} (blue) bound to DMPC-coated (b) 1 μm SSLBs at a molar ratio of 1:100. (c) 100 nm SSLBs at a molar ratio of 1:280.

pathway called sporulation in which a spherical internal organelle, termed the "forespore", is formed that protects the cell's genetic material from environmental insults.[19] SpoVM is among the first coat proteins that localize to the outer surface of the forespore to initiate coat assembly. In 2009, Ramamurthi et al. proposed that SpoVM exploits a novel mechanism for localization to the forespore.[8] Specifically, SpoVM senses, and preferentially binds to, slightly convex curved outer surface of the forespore (~1 μm in diameter), determining its subcellular localization.[8] Recently we dissected the molecular details of its curvature sensing using a SSLB-based *in vitro* fluorescence assay (Figure S1), solution NMR and molecular dynamics simulation.[20] Here we report direct structural studies of SpoVM in SSLBs with native-like curvature.

In solution the C-terminal 11 to 23 residues of SpoVM adopts an amphipathic α-helix that is deeply embedded into the membrane.[20] We rationalized that this is a result of its atypical helical structure that presents a large hydrophobic surface with only one positively charged residue, Arg17, on its polar face when bound to the membrane. As an initial test of this hypothesis, we replaced Arg17 with Asp (SpoVM^{R17D}) and determined that this variant mislocalized *in vivo*.[20] Structurally, SpoVM^{R17D} adopts a similar α-helical structure to the wild-type protein in the presence of liposomes, as judged by circular dichroism (Figure S2). The loss of *in vivo* activity of SpoVM^{R17D} could be due to perturbations in its membrane insertion depth, as a consequence of losing the "snorkeling" effect of the Arg upon replacement with the Asp.[21] To address this, we compared the insertion depths of wild-type and R17D SpoVM variant using HRMAS spectroscopy and 1 μm SSLBs with native forespore-like curvature. Figure 2a shows a representative 1D ^{1}H HRMAS spectrum of DMPC lipids coating 1 μm silicon beads. Despite a relatively small volume fraction of lipid bilayers of these large SSLBs (~0.2 mg lipids on 20 mg beads in a Bruker 4 mm rotor insert), proton direct detection provided sufficient sensitivity to observe the lipid resonances. Furthermore, the spectrum displayed high resolution, which is a result of the flexibility of fluid lipids of these SSLBs. Multiple protons from the lipid headgroup, glycerol backbone, and fatty acid chains were well-resolved at the moderate sample spinning speed of 10 kHz. Since these proton resonances reflect different membrane depths, they are ideal for monitoring the localization of specific protein–lipid interactions as a function of membrane curvature.

To define the membrane insertion depth of SpoVM and SpoVM^{R17D}, we exploited the saturation transferred difference (STD) NMR experiment. In our protein–lipid preparations the spin-diffusion process is very fast among protein protons, but it is slow between lipid protons that reside in different regions of the bilayer such as the headgroup, glycerol backbone, and acyl chains since it is mainly an intermolecular process.[22−24] Under these conditions, selectively saturating protein aromatic resonances rapidly equilibrates protein protons, and the degree of transfers between protein and lipid protons reflects their averaged proximity. The STD effects for SpoVM and SpoVM^{R17D} peptides bound to 1 μm DMPC-coated SSLBs are shown in Figure 2b. For SpoVM, the maximum STD factor was on lipid H3 protons with substantial effects on the methyl and methylene protons of acyl chains and smaller effects on the headgroups. Conversely, the largest effect for SpoVM^{R17D} was on lipid H4 protons and on protons of the glycerol backbone and headgroups, but only minimal transfer to the methyl and methylene protons of acyl chains. Thus, these data supported a model in which SpoVM inserts deeply into the membrane with its hydrophobic side chains interacting with lipid acyl chains, while SpoVM^{R17D} insertion is shallower, due to the shorter and negatively charged Asp side-chain, mainly interacting with lipid head groups and glycerol backbones.

To examine whether membrane curvature affects insertion depth of these proteins, we collected STD data on highly curved 100 nm DMPC-coated SSLBs (Figure 2c). On this membrane, both SpoVM and SpoVM^{R17D} peptides showed similar large STD effects on protons in the lipid glycerol backbone and headgroup, suggesting shallow penetration. Further, at higher protein/lipid ratios, substantial reductions in resonance intensity as a result of increased line broadening were consistently seen on choline methyl protons upon peptide binding (Figure S3). Together, the results indicated that SpoVM and SpoVM^{R17D} only shallowly insert into highly curved bilayers. Thus, our data provided direct experimental support that curvature can regulate insertion depth of membrane proteins, which in turn regulate protein activities.[25−29]

We further sought to validate our solution NMR results, which were performed in planar bicelles, in the more native-like lipid environments of SSLBs. Figure 3 shows 2D high-resolution ^{13}C–^{13}C correlation spectra of SpoVM and SpoVM^{P9A}, a functionally impaired variant that does not

DOI: 10.1021/jacs.5b08303
J. Am. Chem. Soc. 2015, 137, 14031−14034

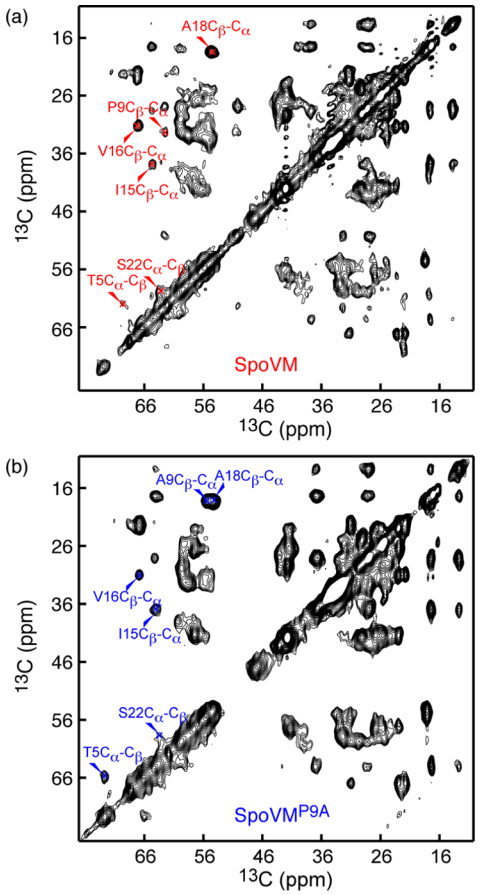

Figure 3. Structure validations of SpoVM and SpoVM^{P9A} in SSLBs. 2D MAS $^{13}C-^{13}C$ correlation spectra for ^{13}C-,^{15}N-labeled SpoVM (a) and SpoVM^{P9A} (b) bound to DMPC-coated 50 nm SSLBs. The data were collected on an 800 MHz Bruker NMR instrument with 35 ms mixing time,10 kHz spinning speed, 1.5 s recycle delay at 15 °C (sample temperature) for increased spectral sensitivity. The total acquisition time was about 36 h. Temperature-dependent static ^{31}P NMR spectra indicate no lipids are detached from these SSLBs to form small discoidal structures in the gel phase (Figure S4).

specifically recognize membrane curvature *in vivo* and *in vitro*. Both peptides can bind to the highly curved 50 nm DMPC-coated SSLBs. Based on their characteristic chemical shifts, several resonances of SpoVM and SpoVM^{P9A} were readily assigned (Figure 3a,b); their C_α secondary shifts (red in Figure S5) are in agreement with their secondary shifts observed in isotropic bicelles (black in Figure S5). In addition, Ala9 C_α and C_β chemical shifts at 55.5 and 18.2 ppm and the change of Thr5 resonance positions from 62.2 and 69.5 ppm for SpoVM to 65.9 and 72.8 ppm for SpoVM^{P9A} were consistent with a structural rearrangement of N-terminal residues from a loop in SpoVM to an α-helical conformation in SpoVM^{P9A}. These data support our earlier conclusion that disruption of SpoVM helix by Pro9 is necessary for SpoVM curvature sensing.[20]

An overlay of SpoVM spectra bound to SSLBs and liposomes showed remarkably similarity and comparable resolution (Figure S6). These observations indicate that the presence of a support does not affect the protein structure. The stability of SSLBs during sample spinning is validated by their typical chemical shift powder patterns of the static ^{31}P spectra collected before and after MAS experiments (Figure S7). Furthermore, SpoVM binding does not alter the bilayer structure (Figure S8), since SpoVM only functions as a curvature-sensing molecule and does not tabulate or vesiculate membranes. Together, these observations indicate that SSLBs are suitable for structural studies by MAS ssNMR.

In summary, our study demonstrates that SSLBs are an effective model system for structural and topological characterization of membrane geometry-sensitive molecules by MAS ssNMR. The spectral resolution is comparable to that from liposomes, and spectral sensitivity is adequate for studying protein−lipid and lipid−lipid interactions. Furthermore, we provide direct experimental evidence that bilayer curvature can affect the insertion depth of peripheral membrane proteins.

■ ASSOCIATED CONTENT

Supporting Information

The Supporting Information is available free of charge on the ACS Publications website at DOI: 10.1021/jacs.5b08303.

Detailed experimental procedures, fluorescence, CD, ^1H HRMAS, static ^{31}P, and $^{13}C-^{13}C$ correlation spectra for SpoVM and variants (PDF)

■ AUTHOR INFORMATION

Corresponding Author

*ftian@psu.edu

Author Contributions

⊥These authors (R.F. and R.L.G., Jr.) contributed equally.

Notes

The authors declare no competing financial interest.

■ ACKNOWLEDGMENTS

We thank Drs. T. A. Cross and K. C. Huang for helpful discussions, and Nissan Chemical Industries, Ltd. for 50 and 100 nm silicon beads. The MAS ssNMR data were performed at the National High Magnetic Field Laboratory, which is supported by NSF Cooperative Agreement no. DMR-1157490, the State of Florida, and the U.S. Department of Energy. This work was supported by the National Institutes of Heath NIGMS (R01GM105963 to F.T. and R01GM094526 to J.M.F.) and the NIH Intramural Research Program, National Cancer Institute, Center for Cancer Research (K.S.R.)

■ REFERENCES

(1) McMahon, H. T.; Gallop, J. L. *Nature* **2005**, *438*, 590−596.
(2) Groves, J. T.; Kuriyan, J. *Nat. Struct. Mol. Biol.* **2010**, *17*, 659−665.
(3) Melikyan, G. B. *Curr. Opin. Virol.* **2014**, *4*, 1−7.
(4) Schlame, M.; Acehan, D.; Berno, B.; Xu, Y.; Valvo, S.; Ren, M.; Stokes, D. L.; Epand, R. M. *Nat. Chem. Biol.* **2012**, *8*, 862−869.
(5) Bigay, J.; Gounon, P.; Robineau, S.; Antonny, B. *Nature* **2003**, *426*, 563−566.
(6) Lenarcic, R.; Halbedel, S.; Visser, L.; Shaw, M.; Wu, L. J.; Errington, J.; Marenduzzo, D.; Hamoen, L. W. *EMBO J.* **2009**, *28*, 2272−2282.
(7) Ramamurthi, K. S.; Losick, R. *Proc. Natl. Acad. Sci. U. S. A.* **2009**, *106*, 13541−13545.
(8) Ramamurthi, K. S.; Lecuyer, S.; Stone, H. A.; Losick, R. *Science* **2009**, *323*, 1354−1357.
(9) Rangamani, P.; Lipshtat, A.; Azeloglu, E. U.; Calizo, R. C.; Hu, M. F.; Ghassemi, S.; Hone, J.; Scarlata, S.; Neves, S. R.; Iyengar, R. *Cell* **2013**, *154*, 1356−1369.
(10) Schmick, M.; Bastiaens, P. I. H. *Cell* **2014**, *156*, 1132−1138.
(11) Shen, H. Y.; Pirruccello, M.; De Camilli, P. *Cell* **2012**, *150*, 1300−U226.
(12) Walde, P.; Cosentino, K.; Engel, H.; Stano, P. *ChemBioChem* **2010**, *11*, 848−865.

DOI: 10.1021/jacs.5b08303
J. Am. Chem. Soc. 2015, 137, 14031−14034

(13) Bayerl, T. M.; Bloom, M. *Biophys. J.* **1990**, *58*, 357−362.
(14) Buranda, T.; Huang, J.; Ramarao, G. V.; Ista, L. K.; Larson, R. S.; Ward, T. L.; Sklar, L. A.; Lopez, G. P. *Langmuir* **2003**, *19*, 1654−1663.
(15) Savarala, S.; Ahmed, S.; Ilies, M. A.; Wunder, S. L. *Langmuir* **2010**, *26*, 12081−12088.
(16) Galneder, R.; Kahl, V.; Arbuzova, A.; Rebecchi, M.; Radler, J. O.; McLaughlin, S. *Biophys. J.* **2001**, *80*, 2298−2309.
(17) Picard, F.; Paquet, M. J.; Dufourc, E. J.; Auger, M. *Biophys. J.* **1998**, *74*, 857−868.
(18) Levin, P. A.; Fan, N.; Ricca, E.; Driks, A.; Losick, R.; Cutting, S. *Mol. Microbiol.* **1993**, *9*, 761−771.
(19) Tan, I. S.; Ramamurthi, K. S. *Environ. Microbiol. Rep.* **2014**, *6*, 212−225.
(20) Gill, R. L.; Castaing, J. P.; Hsin, J.; Tan, I. S.; Wang, X.; Huang, K. C.; Tian, F.; Ramamurthi, K. S. *Proc. Natl. Acad. Sci. U. S. A.* **2015**, *112*, E1908−E1915.
(21) Strandberg, E.; Killian, J. A. *FEBS Lett.* **2003**, *544*, 69−73.
(22) Yau, W. M.; Gawrisch, K. *J. Am. Chem. Soc.* **2000**, *22*, 3971−3972.
(23) Soubias, O.; Gawrisch, K. *J. Am. Chem. Soc.* **2005**, *127*, 13110−13111.
(24) Aucoin, D.; Camenares, D.; Zhao, X.; Jung, J.; Sato, T.; Smith, S. O. *J. Magn. Reson.* **2009**, *197*, 77−86.
(25) Qiang, W.; Sun, Y.; Weliky, D. P. *Proc. Natl. Acad. Sci. U. S. A.* **2009**, *106*, 15314−15319.
(26) Ambroso, M. R.; Hegde, B. G.; Langen, R. *Proc. Natl. Acad. Sci. U. S. A.* **2014**, *111*, 6982−6987.
(27) Strandberg, E.; Zerweck, J.; Wadhwani, P.; Ulrich, A. S. *Biophys. J.* **2013**, *104*, L09−L11.
(28) Wang, T.; Cady, S. D.; Hong, M. *Biophys. J.* **2012**, *102*, 787−794.
(29) Soubias, O.; Teague, W. E.; Hines, K. G.; Gawrisch, K. *Biochimie* **2014**, *107*, 28−32.

DOI: 10.1021/jacs.5b08303
J. Am. Chem. Soc. 2015, 137, 14031−14034